IEEE Photonics Journal
An IEEE Photonics Society Publication

Open Access

Efficient and Tunable 1.6-μm MgO:PPLN Optical Parametric Oscillator Pumped by Nd:YVO_4/YVO_4 Raman Laser

Volume 12, Number 1, February 2020

Lei Zhao
Xin Ding
Jian Liu
Guizhong Zhang
Xuanyi Yu
Yang Liu
Bing Sun
Jingbo Wang
Yuntao Bai
Guoxin Jiang
Peng Lei
Tengteng Li
Liang Wu
Jianquan Yao

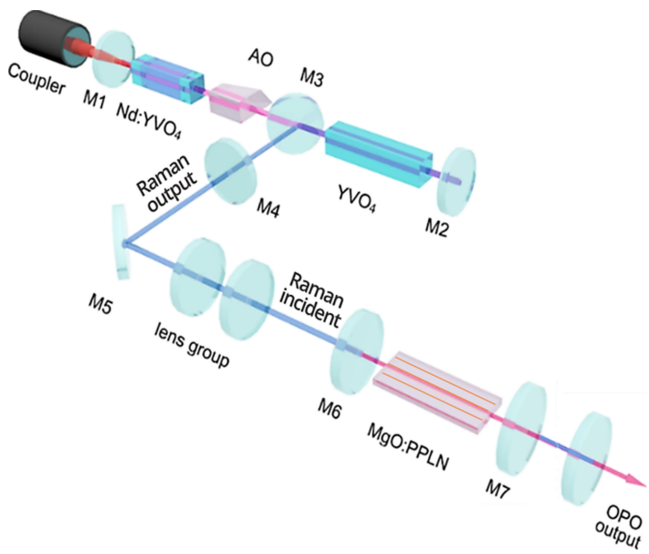

DOI: 10.1109/JPHOT.2019.2955862

Efficient and Tunable 1.6-μm MgO:PPLN Optical Parametric Oscillator Pumped by Nd:YVO_4/YVO_4 Raman Laser

Lei Zhao,[1] Xin Ding,[1] Jian Liu,[1] Guizhong Zhang,[1] Xuanyi Yu,[2] Yang Liu,[1] Bing Sun,[1] Jingbo Wang,[1] Yuntao Bai,[1] Guoxin Jiang,[1] Peng Lei,[1] Tengteng Li,[1] Liang Wu,[1] and Jianquan Yao[1]

[1]Institute of Laser and Opto-Electronics, School of Precision Instrument and Opto-Electronics Engineering and Key Laboratory of Opto-Electronics Information Technology, Ministry of Education, Tianjin University, Tianjin 300072, China
[2]College of Physics Science, Nankai University, Tianjin 300071, China

DOI:10.1109/JPHOT.2019.2955862

Manuscript received September 18, 2019; revised November 17, 2019; accepted November 21, 2019. Date of publication December 5, 2019; date of current version January 7, 2020. This work was supported by the National Natural Science Foundation of China under Grants 11674242 and 11674243.
Corresponding author: Xin Ding (e-mail: dingxin@tju.edu.cn).

Abstract: A highly-efficient tunable 1.6 μm MgO:PPLN-OPO, which we believe to be the first one pumped by a diode-end-pumped Raman laser, is demonstrated. A good beam-quality of actively Q-switched Nd:YVO_4/YVO_4 Raman laser at 1176 nm and a good mode matching of the whole system resulted in a high-performance OPO. The highest Raman-to-signal conversion efficiency was 49.5% at 1638.8 nm when the incident Raman power was 2 W. The maximum output power of 3.2 W at 1663.5 nm with the pulse-width of 2.85 ns was obtained pumped by 7.57-W Raman laser. Meanwhile, the linewidth was less than 0.3 nm and a high beam quality with M^2 factor of 1.92 was obtained.

Index Terms: Beam quality, optical parametric oscillator, raman pumping, 1.6-μm laser.

1. Introduction

1.6-μm eye-safe laser sources, located in atmospheric transmission window covering methane-absorption lines, are attractive in applications of laser ranging, Doppler wind radar, and trace methane gas detection [1]–[3]. At present, the laser generation around 1.6-μm band is obtained by methods such as Er^{3+}-doped fiber/crystalline lasers and Raman lasers [4]–[6]. Another effective approach for narrow-pulse-width (about several nanosecond) and high-pulse-energy eye-safe laser sources is based on optical parametric oscillators (OPOs), which is not feasible by means of Er^{3+}-doped fiber lasers and fiber-based Raman lasers [7]–[9]. The OPO performance depends largely on the pump beam-quality. According to the OPO theoretical model proposed by Brosnan *et al*, the threshold of OPO is affected by pump beam-quality, and it can be significantly increased if the pump beam-quality is nonuniform [10], [11]. Besides, mode matching, which is also subjected to the pump beam quality, impacts the conversion efficiency of OPO. The common pump source of OPOs is the near-infrared solid-state laser at 1.06 μm (e.g., Nd:YVO_4 lasers). In contrast, solid-state Raman lasers at 1.17 μm (with Raman shift of 890 cm^{-1} based on 1.06 μm), owing to Raman beam clean-up effect, are able to generate a higher beam quality light radiation with narrow pulse width and high peak power [12], [13]. Moreover, the Raman process is less sensitive

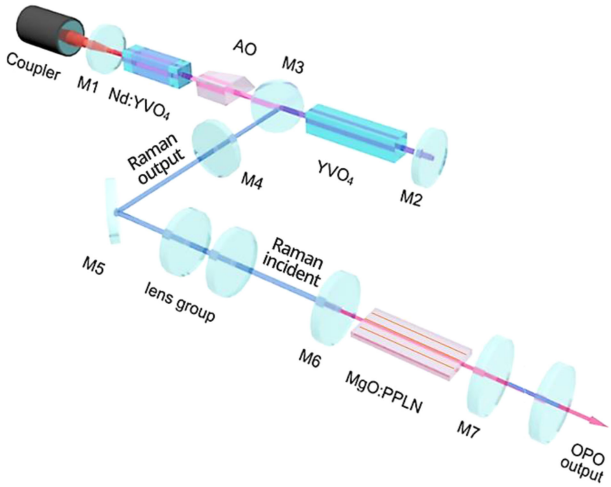

Fig. 1. Schematic diagram of the singly resonant OPO pumped by an actively Q-switched Nd:YVO_4/YVO_4 folded coupled cavity Raman laser at 1176 nm.

to thermal variations that can lead to dephasing and also less sensitive to angular misalignments, and Raman light has a narrower line width. Therefore, using solid-state Raman lasers as pump source is a promising way to get high-performance tunable OPOs. OPO pumped by Raman laser, combining different nonlinear frequency conversion techniques, is a flexible and reliable technique to expand the laser wavelength.

In 2011, Bai *et al.* first reported a KTP-OPO pumped within an YAG/$SrWO_4$ Raman laser and output power of 485 mW at 1810 nm with laser diode (LD)-to-signal conversion efficiency of 6.75% were obtained [14]. Recently, Zhu *et al.* demonstrated a KTA-OPO intracavity pumped by a Nd:YVO_4 self-Raman laser, and the output power at 1742 nm was 1.2 W [15]. Although the Raman intracavity pumping scheme can take a good use of high power density, the insertion of the OPO nonlinear crystal and the OPO process can impact the mode of the Raman beam within cavity, which is harmful for the mode matching [14]. The Raman external-cavity pumping method are easier to get better mode matching and higher conversion efficiency, because the Raman laser and the OPO can be optimized separately.

In this paper, we present a high efficiency and tunable MgO:PPLN OPO around 1.6-μm using Raman external-cavity pumping configuration. An active Q-switched Nd:YVO_4/YVO_4 Raman laser at 1176 nm based on a folded coupled cavity was used as pump source, which could provide high power and high beam-quality Raman output. In addition, the mode size of the Raman beam could well match the signal beam by using external-cavity pumping configuration. The OPO signal tuning range was 1602.9$\sim$1663.5 nm as the crystal grating periods changing from 29.08 to 30.49 μm. The highest Raman-to-signal conversion efficiency was 49.5% at 1638.8 nm when the incident Raman power was 2 W. The average output power of 3.2 W at 1663.5 nm with pulse width of 2.85 ns was obtained under the incident Raman power of 7.57 W. The linewidth of 1663.5 nm was less than 0.3 nm and the M^2 factor was 1.92. To the best of our knowledge, this is the first report about MgO:PPLN-OPO pumped by Raman laser and the highest signal output power amongst ever-reported OPOs pumped by Raman laser. This high performance OPO by using Raman laser as a pump source, has great prospect for applications of laser ranging, Doppler wind radar, and trace methane gas detection.

2. Experimental Arrangement and Analysis

The experiment configuration of the PPLN-OPO pumped by a Raman laser at 1176 nm is depicted in Fig. 1. A self-assembled active Q-switched Nd:YVO_4/YVO_4 coupled cavity Raman laser were employed to pump the follow-up OPO.

In an active Q-switched Nd:YVO_4/YVO_4 folded cavity Raman laser, an 880 nm fiber-coupled LD (core diameter $\varphi = 400$ μm and numerical aperture NA $= 0.22$) was used as the pump source. Pump beams were focused to the laser crystal by a 1:1 multi-lens coupler, forming a spot radius of 200 μm near the incident facet. Laser crystal with size of $3 \times 3 \times 20$ mm^3 was an *a*-cut composite crystal, with a 16-mm 0.3-at% Nd:YVO_4 segment in middle and 2-mm YVO_4 segments on each end, which was wrapped in indium foil and mounted in a water-cooled aluminum holder maintained at 12 °C. Both facets of the laser crystal were coated for high-transmission (HT) at 880 nm (T $>$ 99%) and 1064 nm (T $>$ 99.9%). Raman crystal was an *a*-cut YVO_4 with size of $3 \times 3 \times 30$ mm^3, coated for HT (T $>$ 99.5%) at 1064 nm and 1176 nm on each facet. The 20-mm-long acousto-optic Q-switch (Gooch&Housego, I-QS080-1C10G-8-GH28) driven at 80-MHz ultrasonic frequency was also employed, with HT (T $>$ 99.6%) coating at 1064 nm on both facets. Both Raman crystal and Q-switch were cooled by refrigerant water maintained at 18 °C. A folded coupled cavity was employed to optimize beam propagations of fundamental and Stokes resonators respectively [16]. The plane-concave mirror M1 with 200-mm radius of curvature (ROC) was coated for HT at 880 nm (T $>$ 99%) and high-reflective (HR) at 1064 nm (R $>$ 99%), and flat mirror M2 was coated for HR (R $>$ 99%) at both 1064 nm and 1176 nm. The length of fundamental cavity consisting of M1 and M2 was 130 mm. M3 (45° folded mirror) was coated for HT at 1064 nm and HR at 1176 nm to separate Raman and fundamental resonators. The concave mirror M4 (ROC $=$ 100 mm) was an output coupler with partial-transmission (T $=$ 18%) at 1176 nm. The length of Raman cavity consisting of M2 and M4 was 70 mm.

The output Raman laser at 1176 nm was used as a pump light for OPO. The 45° mirror M5 was coated for HT at 1064 nm and HR at 1176 nm. A waist radius of pump beam about 87–90 μm in MgO:PPLN crystal was achieved via convex lens group (f1 $=$ 200 mm, f2 $=$ 300 mm). The 5%MgO:PPLN crystal was $1 \times 5 \times 35$ mm^3 in size, with four grating periods of 29.08, 29.52, 29.98 and 30.49 μm, and it was coated for HT at 1064 nm (T $>$ 99%), 1176 nm (T $>$ 99%), and 1300–1800 nm (T $>$ 98.5%) on both facets. MgO:PPLN crystal was mounted in a servo-controlled oven, and we changed grating periods by lateral movement. Compared with the undoped PPLN, damage threshold of 5%MgO doped PPLN has a substantial increase. The OPO resonator was formed by two concave mirrors M6 (ROC $=$ 50 mm) and M7 (ROC $=$ 50 mm). M6 was coated for HT at 1176 nm (T $>$ 95%) and HR at 1600–1680 nm (R $>$ 99.5%). M7 was coated for HT at 1176 nm (T $>$ 98%) and PT (T $=$ 11%$\sim$17%) at 1600–1680 nm. Both M6 and M7 were made of K9 glass, which had an intense absorption at the idler range. Pump, signal, and idler waves were all *e*-polarized to utilize the highest nonlinear coefficient d_{33} ($\sim$25 pm/V) in MgO:PPLN crystal and the corresponding effective nonlinear coefficient d_{eff} ($d_{\mathrm{eff}} = 2d_{33} / \pi = 16$ pm/V). After M7, a flat mirror, also made of K9 glass, with coating for HR at 1176 nm and HT at 1600–1680 nm, was placed to filter residual pump and idler waves.

Mode matching in the whole system was considered and optimized. In Raman laser, we first considered the thermal lens effect of both the laser crystal and the Raman crystal which could seriously affect beam distributions. Given the LD pump power of 39.8 W at 880 nm, the thermal focal length in the Nd:YVO_4 crystal (with measured absorption coefficient of 0.92 cm^{-1} at 880 nm) was $\sim$170 mm [17], while in the YVO_4 crystal it was $\sim$100 mm based on Eq. (30) in Ref. [18]. Fundamental and Raman beam distributions were simulated according to ABCD transmission matrix and shown in Fig. 2(a) and 2(b). The 130-mm-long fundamental cavity and the 70-mm-long Raman cavity were employed, and in the laser crystal, the beam waist radius of fundamental was $\sim$200 μm which could match well with the LD pump beam waist radius of 200 μm. Radii of fundamental and Raman beams were $\sim$125 μm and $\sim$130 μm in YVO_4 crystal, respectively, so a good mode matching could be achieved between fundamental and Raman beams in the Raman crystal. In OPO, signal (1603 and 1663 nm) beam distributions in 45-mm-long OPO resonator with 50 mm ROC of mirrors M6 and M7, were simulated according to ABCD transmission matrix. Results were indicated by the red and green (above but very near the red line) lines in Fig. 2(c). Radii of signal beams were about 105$\sim$110 μm in the MgO:PPLN crystal. The pump beam was mode matched to the signal beams in the OPO crystal via lens f1 $=$ 200 mm and f2 $=$ 300 mm,

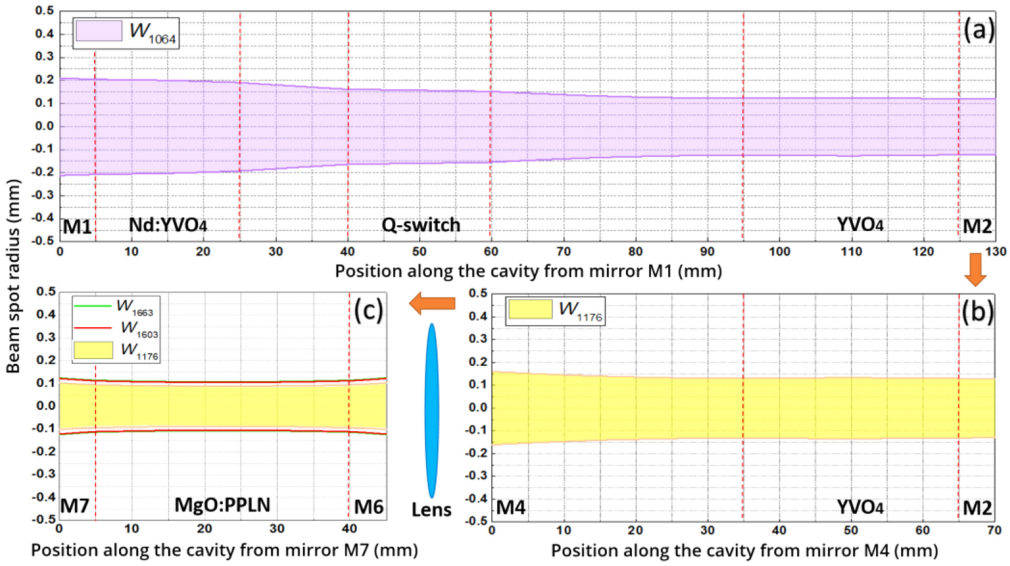

Fig. 2. Beam distributions in (a) fundamental resonator and (b) Raman resonator under LD pump power of 39.76 W at 880 nm. Beam distributions in (c) OPO resonator under incident Raman power of 7.57 W at 1176 nm.

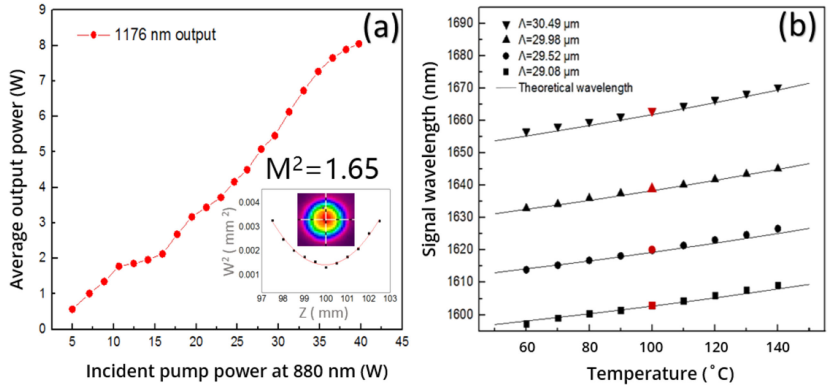

Fig. 3. (a) Average output power at 1176 nm as functions of LD pump power at PRF of 40 kHz and beam profile at 1176 nm under LD pump power of 39.76 W. (b) Wavelength coverage of the Raman laser pumped MgO:PPLN-OPO with the temperature tuning under different grating periods. Theoretical simulation values based on Eq. (2) and (4) in Ref. [20] and parameters in Ref. [21] shown as solid lines. Experimental values shown as points.

producing a waist radius of 90 μm in MgO:PPLN crystal, corresponding the focusing parameter $\xi = 0.4$, where $\xi = L/b$, L is the crystal length and $b = 2\pi w^2 n/\lambda$ is the confocal parameter, and it was indicated by the yellow area in Fig. 2(c).

3. Results and Discussion

Firstly, the output performance of the Raman laser was investigated. The output power of Stokes at 1176 nm as function of LD pump power is shown in Fig. 3(a). A maximum output power of Raman laser was 8.05 W under the LD pump power of 39.76 W at pulse repetition frequency (PRF) of 40 kHz, corresponding to LD-to-Raman conversion efficiency of 20.2%. Meanwhile, the

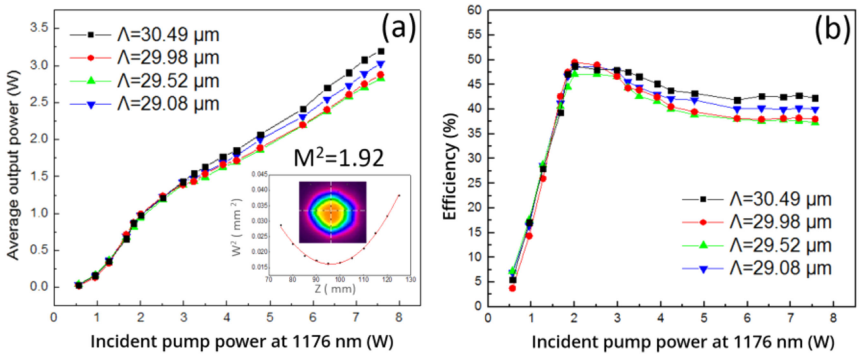

Fig. 4. Signal (a) output powers and (b) Raman-to-signal conversion efficiencies as functions of incident Raman power with different grating periods. The inset is the signal beam profile at incident power of 7.57 W.

pulse width was 4.58 ns and the peak power was 44 kW. The M^2 factor of Stokes measured by the knife-edge method was about 1.65 at maximum output power and corresponding spatial beam profile is shown as the inset of Fig. 3(a). Using separate laser crystal and Raman crystal could disperse the thermal load and realize good mode matching based on the folded coupled cavity, which resulted in high output power of Raman laser, coincident with other reports in similar cases [16], [19]. The Raman laser with both high output power and high beam-quality could be used as a good pump source for the OPO experiments. However, the maximum incident Raman power at 1176 nm for MgO:PPLN OPO was 7.57 W due to the coupling loss of M5 and lens group.

The tuning ranges of the MgO:PPLN OPO pumped by Raman laser at 1176 nm were measured by an optical spectrum analyzer (Yokogawa AQ6370D). With the working temperature changing from 60 °C to 140 °C, the signal tuning ranges were measured from 1597.3 to 1609.2 nm, 1613.9 to 1626.6 nm, 1632.9 to 1645.1 nm and 1656.6 to 1670.3 nm under grating periods of 29.08, 29.52, 29.98 and 30.49 μm, respectively. Corresponding theoretical simulation values were 1598 to 1608 nm, 1614 to 1625 nm, 1633 to 1645 nm and 1655 to 1669 nm, respectively. Fig. 3(b) shows that the experimental results of wavelength tuning range agreed well with the theoretical values, and the minor deviations were determined by the inherent error of crystal grating-period and accuracy of temperature-control. The idler lights, which were expected about from 3975 nm to 4437 nm, were not observed because of the intense absorption in K9 mirrors.

The output characteristics of the MgO:PPLN OPO with different grating periods at PRF of 40 kHz are shown in Fig. 4, when the temperature of the MgO:PPLN crystal were fixed at 100 °C. The grating-periods were 29.08, 29.52, 29.98 and 30.49 μm, corresponding to the signal wavelengths of 1602.9, 1619.9, 1638.8, and 1663.5 nm, respectively. Corresponding transmittances of output coupler M7 at different signal wavelengths were T1603 = 13.0%, T1620 = 11.5%, T1639 = 11.5%, and T1663 = 16.3%. As shown in Fig. 4(a), the OPO began to oscillate when the incident Raman power at 1176 nm was around 500 mW. The output powers of different signal waves were almost the same at lower incident Raman power and their difference increased with the rising incident Raman power, due to various transmittances. The maximum signal output power at 1663.5 nm was 3.2 W under the maximum incident Raman power of 7.57 W, which is the highest signal output power amongst ever-reported OPOs pumped by a Raman laser. The corresponding Raman-to-signal conversion efficiency was 42.3% and LD-to-signal conversion efficiency was 8.05%. The beam quality M^2 factor of signal beam was about 1.92 at maximum power of 3.2 W and the beam profile is shown in the inset of Fig. 4(a). The maximum output powers at other three signals (1602.9, 1619.9, and 1638.8 nm) were 3.02, 2.82, and 2.88 W, corresponding to the Raman-to-signal conversion efficiencies of 40.0%, 37.3%, and 38.0%, respectively. It should be noted that the output power at 1638.8 nm (Λ = 29.98 μm) was higher than it was at 1619.9 nm (Λ = 29.52 μm) with the same transmittances (T = 11.5%). The reason was that a higher

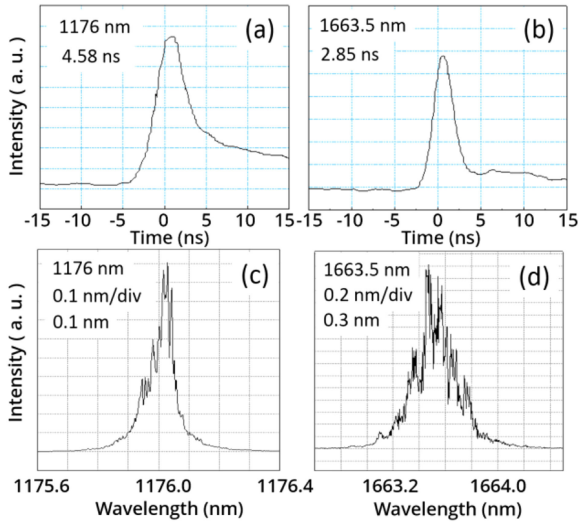

Fig. 5. Typical oscilloscope trace at (a) 1176 nm and (b) 1663.5 nm at the maximum LD pump power. Fine spectrum at (c) 1176 nm and (d) 1663.5 nm at the maximum LD pump power.

parametric gain was obtained at 1638.8 nm due to larger grating-period, when the transmittance and incident Raman power density were the same according to the gain calculation formula of OPO [22]. Fig. 4(b) shows the conversion efficiencies of different signals versus the incident Raman power at 1176 nm. The maximum Raman-to-signal conversion efficiencies at different signals (1602.9, 1619.9, 1638.8, and 1663.5 nm) were 48.6%, 47.1%, 49.5%, and 48.8%, which were both at the incident Raman power of 2 W. We attributed it to a good Raman beam quality ($M^2 = 1.2$) and evenly distributed power intensity of Stokes, which were due to Raman clean-up effect and favored a good matching between pump and signal waves to achieve the high conversion efficiency.

The temporal characteristics of incident Raman and signal waves were investigated using a photoelectric detector (Thorlabs DET08C) and an oscilloscope (Tektronix DPO2024B). The temporal traces of signal at 1663.5 nm and incident Raman at 1176 nm under the maximum LD pump power are shown in Fig. 5(a) and 5(b), when the crystal grating period was fixed at 30.49 μm with the working temperature of 100 °C. Due to the threshold characteristic of OPOs, pulse duration of signal at 1663.5 nm was 2.85 ns, while it of Raman at 1176 nm was 4.58 ns. The corresponding peak power at 1663.5 nm was up to 28.1 kW. The fine spectrum at 1176 and 1663.5 nm were recorded by a spectrometer (Yokogawa AQ6370D) with a resolution of 0.02 nm, depicted in Fig. 5(c) and 5(d). Compared with 1176-nm incident Raman linewidth of ~0.1 nm, 1663.5-nm signal linewidth was spread to ~0.3 nm at the maximum LD pump power, mainly because of the phase mismatch.

4. Conclusion

In conclusion, a highly efficient MgO:PPLN-OPO with tuning range from 1602.9 nm to 1663.5 nm was realized, which was external-cavity pumped by an active Q-switched Nd:YVO_4/YVO_4 Raman laser based on a composite cavity. Due to the high beam quality of Raman laser and good mode matching, the maximum Raman-to-signal conversion efficiency of 49.5% at 1638.8 nm was achieved under the incident Raman power of 2 W. The signal output power at 1663.5 nm was 3.2 W corresponding to peak power of 28.1 kW with the M^2 factor of 1.92 when the incident Raman power was 7.57 W and the PRF was 40 kHz. To the best of our knowledge, this is the first time to pump MgO:PPLN-OPO by using a Raman laser and output power of signal is higher than the ever-reported OPOs pumped by Raman laser. The efficient and tunable OPO has potential applications in laser ranging, Doppler wind radar, and trace methane gas detection.

References

[1] A. Fix *et al.*, "Optical parametric oscillators and amplifiers for airborne and spaceborne active remote sensing of CO_2 and CH_4," *Proc. SPIE*, vol. 8182, Sep. 2011, Art. no. 818206.

[2] Y. M. Duan, H. Y. Zhu, G. Zhang, H. Y. Wang, and Y. J. Zhang, "High-power eye-safe KTA-OPO driven by YVO_4/Nd:YVO_4 composite laser," *Opt. Commun.*, vol. 285, no. 16, pp. 3507–3509, Jul. 2012.

[3] O. Lux, H. Fritsche, and H. J. Eichler, "Trace gas remote sensing by lasers," *Optik*, vol. 8, no. 4, pp. 48–51, Dec. 2013.

[4] N. W. H. Chang, N. Simakov, D. J. Hosken, J. Munch, D. J.Ottaway, and P. J.Veitch, "Resonantly diode-pumped continuous-wave and Q-switched Er:YAG laser at 1645 nm," *Opt. Express*, vol. 18, no. 13, pp. 13673–13678, Jun. 2010.

[5] L. Kotov *et al.*, "Millijoule pulse energy 100-nanosecond Er-doped fiber laser," *Opt. Lett.* vol. 40, no. 7, pp. 1189–1192, Apr. 2015.

[6] J. Liu, D. Shen, H. Huang, C. Zhao, X. Zhang, and D. Fan, "High-power and highly efficient operation of wavelength-tunable Raman fiber lasers based on volume Bragg gratings," *Opt. Express*, vol. 22, no. 6, pp. 6605–6612, Mar. 2014.

[7] O. Kokabee, A. Esteban-Martin, M. Ebrahim-Zadeh, "Efficient, high-power, ytterbium-fiber-laser-pumped picosecond optical parametric oscillator," *Opt. Lett.*, vol. 35, no. 19, pp. 3210–3212, Sep. 2010.

[8] K. Zhong *et al.*, "Widely tunable eye-safe optical parametric oscillator with noncollinear phase-matching in a ring cavity," *Opt. Express*, vol. 27, no. 8, pp. 10449–10455, Apr. 2019.

[9] A. Ly, F. Bretenaker, and C. Siour, "30-Hz-linewidth Watt output power 1.65-μm continuous-wave singly resonant optical parametric oscillator," *Opt. Express*, vol. 25, no. 8, pp. 9049–9060, Apr. 2017.

[10] S. Brosnan and R. Byer, "Optical parametric oscillator threshold and linewidth studies," *IEEE J. Quantum Electron.*, vol. QE-15, no. 6, pp. 415–431, Jun. 1979.

[11] S. Guha, F. J. Wu, and J. Falk, "The effects of focusing on parametric oscillation," *IEEE J. Quantum Electron.*, vol. 18, no. 5, pp. 907–912, May 2003.

[12] J. T. Murray, W. L. Austin, and R. C. Powell, "Intracavity Raman conversion and Raman beam cleanup," *Opt. Mater.*, vol. 11, no. 4, pp. 353–371, Mar. 1999.

[13] P. Jiang *et al.*, "9.80-W and 0.54-mJ actively Q-switched Nd:YAG/Nd:YVO_4 hybrid gain interactively Raman laser at 1176 nm," *Opt. Express*, vol. 25, no. 4, pp. 3387–3393, Feb. 2017.

[14] F. Bai *et al.*, "Efficient 1.8 μm $KTiOPO_4$ optical parametric oscillator pumped within an Nd:YAG/$SrWO_4$ Raman laser," *Opt. Lett.* vol. 36, no. 6, pp. 813–815, Mar. 2011.

[15] H. Zhu *et al.*, "Efficient 1.7 μm light source based on KTA-OPO derived by Nd:YVO_4 self-Raman laser," *Opt. Lett.*, vol. 43, no. 2, pp. 345–348, Jan. 2018.

[16] J. Liu *et al.*, "High-performance second-Stokes generation of a Nd:YVO_4/YVO_4 Raman laser based on a folded coupled cavity," *Opt. Express*, vol. 26, no. 8, pp. 10171–10178, Apr. 2018.

[17] M. E. Innocenzi, H. T. Yura, C. L. Fincher, and R. A. Fields, "Thermal modeling of continuous-wave end-pumped solid-state lasers," *Appl. Phys. Lett.* vol. 56, no. 19, pp. 1831–1833, Jun. 1990.

[18] H. Pask, "The design and operation of solid-state Raman lasers," *Prog. Quantum Electron.*, vol. 27, no. 1, pp. 3–56, 2003.

[19] J. Liu *et al.*, "10.3-W actively Q-switched Nd:YVO_4/YVO_4 folded coupled-cavity Raman laser at 1176 nm," *Appl. Opt.*, vol. 57, no. 12, pp. 3154–3158, Apr. 2018.

[20] D. H. Jundt, "Temperature-dependent Sellmeier equation for the index of refraction n_e in congruent lithium niobate," *Opt. Lett.*, vol. 22, no. 20, pp. 1553–1555, Oct. 1997.

[21] O. Gayer, Z. Sacks, E. Galun, and A. Arie, "Temperature and wavelength dependent refractive index equations for MgO-doped congruent and stoichiometric $LiNbO_3$," *Appl. Phys. B—Lasers Opt.*, vol. 94, no. 2, pp. 367–367, Aug. 2010.

[22] J. A. Armstrong, N. Bloembergen, J. Ducuing, and P. S. Pershan, "Interactions between light waves in a nonlinear dielectric," *Phys. Rev.*, vol. 127, no. 6, pp. 1918–1939, Apr. 1962.